

## Polarization and Differential Cross Section of Neutrons Scattered from $\text{Be}^9$ : Parities of the 7.37- and 7.54-MeV States in $\text{Be}^{10}\dagger$

R. O. LANE, A. J. ELWYN, AND A. LANGSDORF, JR.

Argonne National Laboratory, Argonne, Illinois

(Received 23 August 1963)

The polarization and the differential scattering cross sections for neutrons scattered from  $\text{Be}^9$  were measured at 5 angles for neutron energies from 0.2 to 2.0 MeV. The data are interpreted in terms of a two-channel process. The neutron scattering resonances at 0.625 and 0.815 MeV, corresponding to levels in  $\text{Be}^{10}$  at 7.37 and 7.54 MeV, were assigned the spin and parity values  $J^\pi=3^-$  ( $l=2$ ) and  $J^\pi=2^+$  ( $l=1$ ), respectively. The calculations took account of the effects of  $s$ -wave and  $p$ -wave backgrounds as well as approximate contributions of  $1^-$  and  $2^-$  bound states.

### I. INTRODUCTION

MEASUREMENTS of the neutron total cross sections<sup>1</sup> and differential scattering cross sections<sup>2,3</sup> of  $\text{Be}^9$  for neutrons below 1–2 MeV have so far failed to give unique assignments to the parities of the levels in  $\text{Be}^{10}$  at excitation energies of 7.37 and 7.54 MeV, corresponding to resonances at neutron energies of 0.625 and 0.815 MeV, respectively. Both Willard *et al.*<sup>2</sup> and Lane and Monahan<sup>3</sup> were able to represent differential scattering data near the 0.625-MeV resonance on the assumption that the level has a spin and parity of  $J^\pi=3^+$  and was therefore formed by neutrons with orbital angular momentum  $l=1$ . This fit required rather special assumptions; in particular, it was necessary to assume that the  $s$ -wave background scattering is all in channel spin  $S=1$ . This requirement is in disagreement with the thermal scattering data.<sup>4</sup> Marion<sup>5</sup> has pointed out that the 7.37-MeV state in  $\text{Be}^{10}$  and the 8.89-MeV state in  $\text{B}^{10}$  are probably analog states with isotopic spin  $T=1$  in the mass-10 isobaric triad. From an analysis of data<sup>6</sup> on the  $\text{Be}^9(p,n)\text{B}^9$  reaction, Altman *et al.*<sup>7</sup> have concluded that these analog states have negative parity and that therefore the level at 7.37 MeV in  $\text{Be}^{10}$  should be formed by  $d$ -wave neutrons in the  $\text{Be}^9(n,n)\text{Be}^9$  reaction.

The correct parity for this state is not evident from the resonance shape obtained from the measured differential scattering cross sections alone. The interaction of neutrons with  $\text{Be}^9$  nuclei, which have nonzero spin, may involve many more phase shifts than are possible for zero-spin nuclei. Thus a unique solution, if it can be found at all, requires a more extensive

analysis of more numerous data. Usually, a number of simplifying assumptions must be made to reduce the degree of ambiguity in the problem. At this laboratory extensive measurements of the polarization and differential cross section of neutrons scattered at 5 angles from  $\text{Be}^9$  have been made recently for neutron energies below 2 MeV. It was hoped that the simultaneous analysis of the polarization and differential-scattering data might lead directly to a unique assignment of the parity for the 7.37-MeV state and possibly also for the 7.54-MeV state. This paper will give arguments and calculations pertaining to the parities of these states.

### II. EXPERIMENT

In earlier papers<sup>8</sup> the apparatus and methods of data analysis connected with the experimental arrangement have been discussed extensively. Protons from the Argonne 4-MeV Van de Graaff accelerator are incident on evaporated Li targets where they produce a partially polarized<sup>8,9</sup> neutron beam from the  $\text{Li}^7(p,n)\text{Be}^7$  reaction. The neutrons emerging at an angle of  $51^\circ$  from the proton direction pass through the transverse field of an electromagnet which forms part of the collimator and are incident on the Be scatterer. The scattered neutrons are observed at 5 angles simultaneously by large detectors, each consisting of an array of ten  $\text{B}^{10}\text{F}_3$  counters immersed in an oil moderator and surrounded by a tank of aqueous boron solution serving as a shield and collimator. The left-right asymmetry in the scattering of the partially polarized neutron beam is obtained by measuring the intensity of neutrons at a detector, first with the magnet off and then with a magnetic field sufficient to precess the neutron spins through  $180^\circ$  about the field direction. From these data, one obtains in the usual manner the product  $P_1(\alpha)P(\theta)$  where  $P_1(\alpha)$  and  $P(\theta)$  are the polarizations produced in the  $\text{Li}^7(p,n)\text{Be}^7$  source reaction and in the

<sup>†</sup> Work performed under the auspices of the U. S. Atomic Energy Commission.

<sup>1</sup> C. K. Bockelman, Phys. Rev. **80**, 1011 (1950); C. K. Bockelman, D. W. Miller, R. K. Adair, and H. H. Barschall, Phys. Rev. **84**, 69 (1951).

<sup>2</sup> H. B. Willard, J. K. Bair, and J. D. Kington, Phys. Rev. **98**, 669 (1955).

<sup>3</sup> R. O. Lane and J. E. Monahan, Bull. Am. Phys. Soc. **1**, 187 (1956).

<sup>4</sup> H. Palevsky and R. R. Smith, Phys. Rev. **86**, 604(A) (1952).

<sup>5</sup> J. B. Marion, Phys. Rev. **103**, 713 (1956).

<sup>6</sup> J. H. Gibbons and R. L. Macklin, Phys. Rev. **114**, 571 (1959).

<sup>7</sup> A. Altman, W. M. MacDonald, and J. B. Marion, Nucl. Phys. **35**, 85 (1962).

<sup>8</sup> R. O. Lane, A. Langsdorf, Jr., J. E. Monahan, and A. J. Elwyn, Ann. Phys. (New York) **12**, 135 (1961); A. J. Elwyn and R. O. Lane, Nucl. Phys. **31**, 78 (1962); R. O. Lane, A. J. Elwyn, and A. Langsdorf, Jr., Phys. Rev. **126**, 1105 (1962); A. J. Elwyn, R. O. Lane, and A. Langsdorf, Jr., Phys. Rev. **128**, 779 (1962).

<sup>9</sup> H. R. Striebel, S. E. Darden, and W. Haerberli, Nucl. Phys. **6**, 188 (1958).

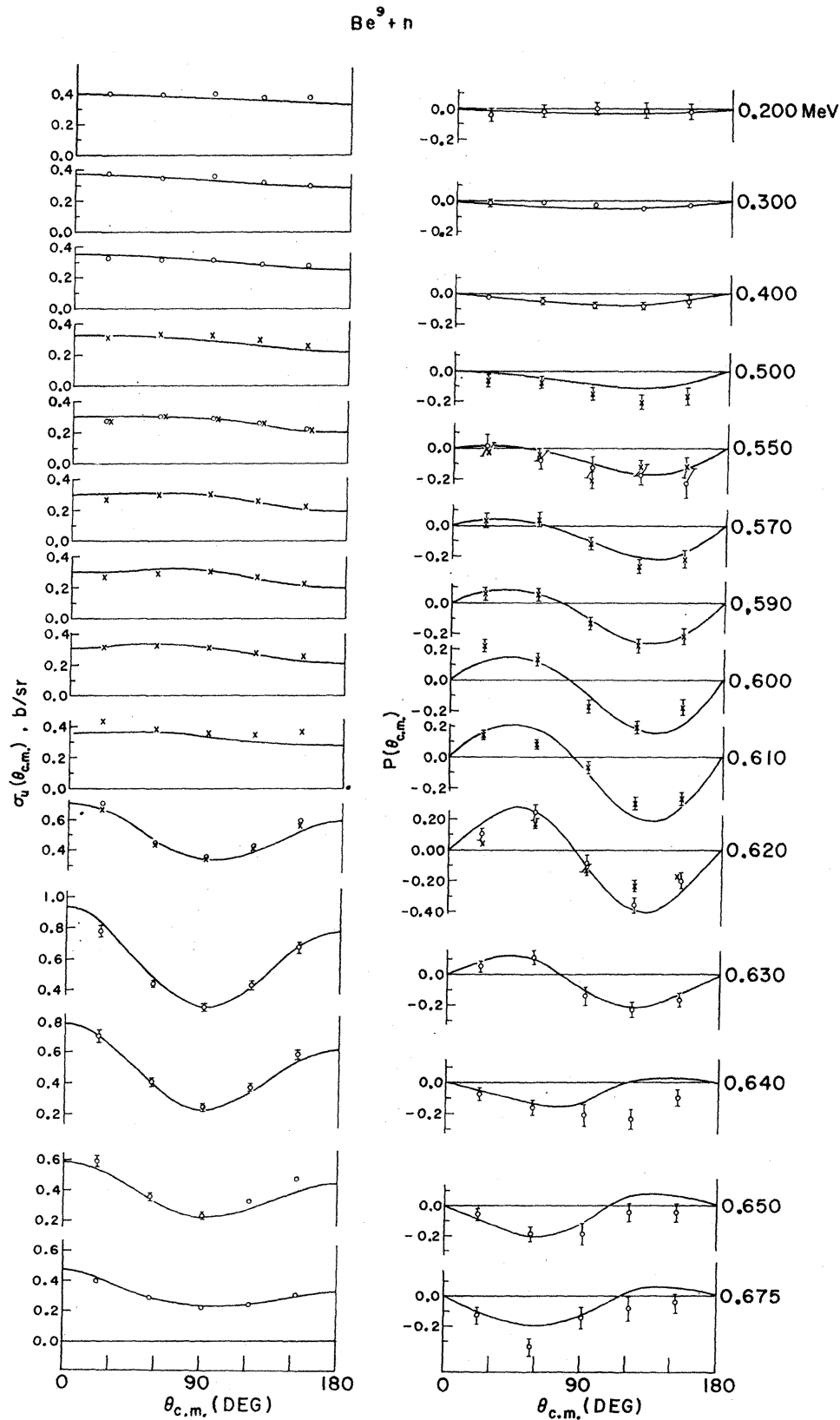


FIG. 1. Angular distributions of the differential scattering cross sections  $\sigma_u(\theta_{c.m.})$  and the polarization  $P(\theta_{c.m.})$  in the center-of-mass system for  $\text{Be}^9+n$ . Neutron energies in the laboratory system (0.200–0.675 MeV) appear on the right. Circles and crosses are experimental points for scatterers  $\frac{1}{8}$  in. and  $\frac{1}{4}$  in. thick, respectively. Where no error bars appear, errors are less than the size of the points. The curves were calculated from the final set of parameters shown in Table I and averaged over the energy spread of the beam.

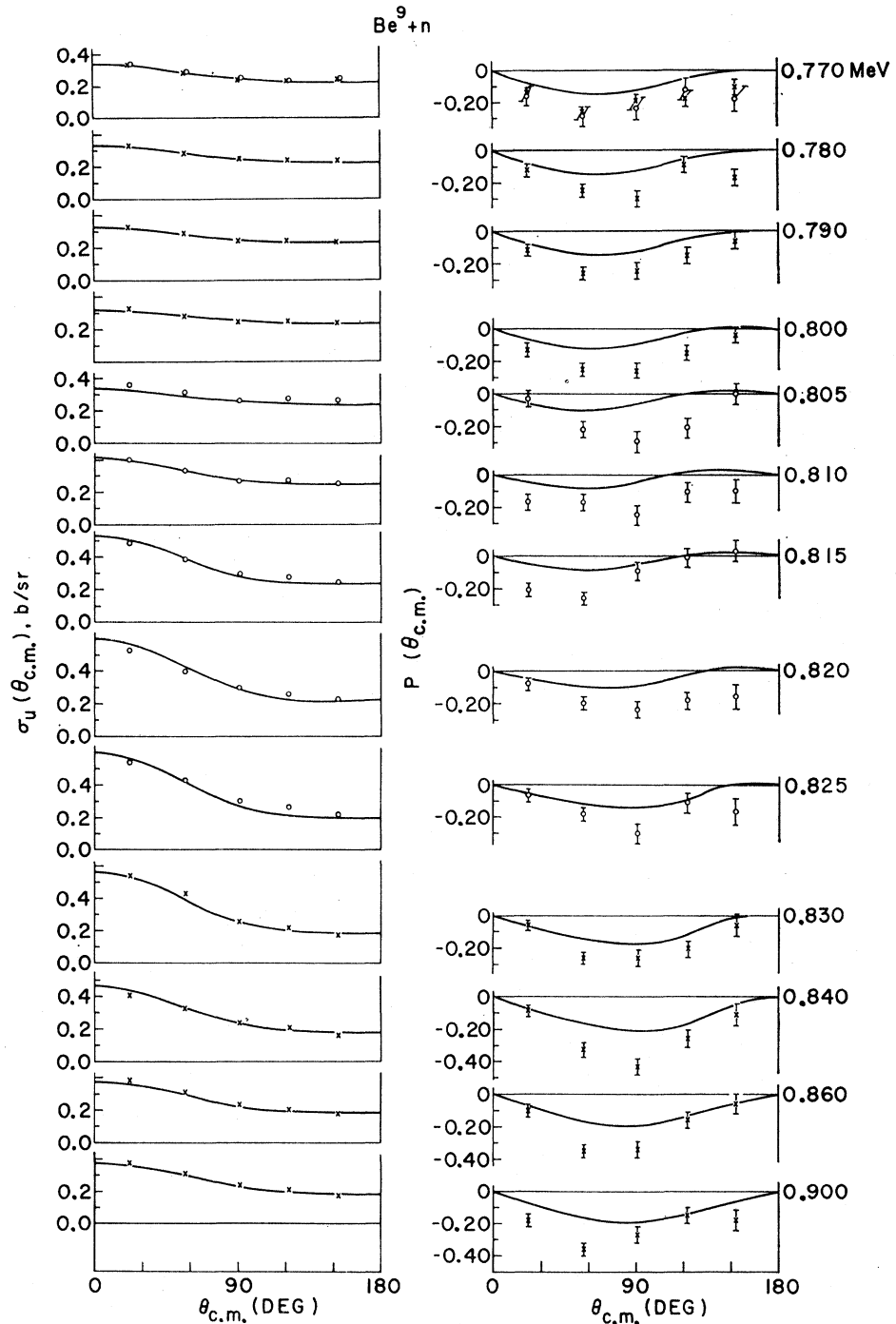


FIG. 2. Angular distributions of the differential scattering cross sections  $\sigma_u(\theta_{c.m.})$  and the polarization  $P(\theta_{c.m.})$  in the center-of-mass system for  $\text{Be}^9+n$ . Neutron energies in the laboratory system (0.770–0.900 MeV) appear on the right. Circles and crosses are experimental points for scatterers  $\frac{1}{16}$  in. and  $\frac{1}{8}$  in. thick, respectively. Where no error bars appear, errors are less than the size of the points. The curves were calculated from the final set of parameters shown in Table I and averaged over the energy spread of the beam.

neutron scattering, respectively. From the known value of  $P_1(51^\circ)$ ,<sup>8,9</sup>  $P(\theta)$  is then deduced for the scatterer. Also, from the same data one obtains the differential scattering cross section  $\sigma_u(\theta)$  for unpolarized neutrons, the numbers of counts being converted to cross section by comparison with the known total cross section for carbon.

The neutrons were incident upon the metallic

beryllium scatterers at an angle of  $45^\circ$ . The scatterers were slabs with linear dimensions 10 in.  $\times$  20 in. and varied in thickness from  $\frac{1}{16}$  in. to  $\frac{1}{8}$  in. The data for  $\sigma_u(\theta)$  were corrected for multiple scattering by means of a Monte Carlo program developed earlier.<sup>10</sup> Because

<sup>10</sup> R. O. Lane and W. F. Miller, Nucl. Instr. Methods 16, 1 (1962).

triple scattering data are needed to properly correct the polarization data for multiple scattering, an approximate correction described previously<sup>8</sup> was made. In addition, the thickness of the samples was minimized to reduce these effects.

Above a neutron energy of about 0.54 MeV, a second group of neutrons from  $\text{Li}^7(p,n)\text{Be}^{7*}$  begins to be produced. These neutrons leaving  $\text{Be}^7$  in its first excited state at 0.43 MeV have been shown by Cranberg<sup>11</sup> to be unpolarized at a proton energy of 3.5 MeV. With the aid of the known relative yields<sup>12</sup> of the first and second groups, corrections were made for the second group on the assumption that it is unpolarized. No inelastic scattering from  $\text{Be}^9$  occurs below 2 MeV. The data for  $\sigma_u(\theta)$  were corrected for the known<sup>8</sup> energy dependence of the detector efficiencies. From the data on the 0.815-MeV resonance, the full energy spread at half-maximum is estimated to be  $\Delta E \approx 20$  keV.

### III. RESULTS

Figures 1 and 2 show the experimental results for  $P(\theta)$  and  $\sigma_u(\theta)$  at the five angles of measurement from 0.2 to 0.9 MeV in the region of interest near the 0.625- and 0.815-MeV resonances. Figure 3 shows  $P(\theta)$  for the range of 1.0 to 2.0 MeV. The  $\sigma_u(\theta)$  in this energy range are not shown but agree with our earlier work.<sup>8</sup> The error bars on the figures include not only statistical errors but also those caused by the uncertainties in the cross-section calibration in the case of  $\sigma_u(\theta)$  and errors in  $P_1(\alpha)$  in the case of  $P(\theta)$ .

The region of most interest here is from 0.5 to 0.9 MeV, which includes the resonances at 0.625 and 0.815 MeV. In this interval the differential cross section was expanded as a sum of Legendre polynomials,

$$\sigma_u(\theta) = \sum_{L=0}^3 B_L P_L(\cos\theta). \quad (1)$$

Similarly, the differential polarization<sup>10</sup> was expanded as a sum of associated Legendre polynomials,

$$\sigma_p(\theta) = \sigma_u(\theta)P(\theta) = \sum_{L=1}^3 C_L P_L^1(\cos\theta). \quad (2)$$

The resulting coefficients  $B_L$  and  $C_L$  are shown as the data points in Figs. 4-6. For  $L \geq 4$ ,  $B_L$  and  $C_L$  are zero within experimental errors and, as can be seen, even  $B_3$  and  $C_3$  are practically zero. The most pronounced resonance structure appears in the terms  $C_2$ ,  $B_0$ , and

$B_2$  near the resonance at 0.625 MeV, and in the  $B_1$  term near 0.815 MeV.

## IV. ANALYSIS AND DISCUSSION

### A. General Discussion

A total angular momentum  $J=3$  for the state at an excitation of 7.37 MeV in  $\text{Be}^{10}$  (corresponding to the 0.625-MeV scattering resonance of  $\text{Be}^9$ ) seems to be well established from measurements of the total cross section and the earlier measurements of the differential cross section. The ground state of  $\text{Be}^9$  has spin  $I=\frac{3}{2}$  and negative parity. Coupling this with the intrinsic spin of the neutron leads to channel spins  $S=I \pm \frac{1}{2} = 1$  or 2. The most probable values of the relative orbital angular momentum  $l$  in the interaction are 0, 1, and 2 at these energies; values of  $l \geq 3$  were not considered. If  $J=3$  is assumed for this state, the coupling  $\mathbf{J}=\mathbf{I}+\mathbf{S}$  precludes  $l=0$  and allows the state to be formed by neutrons with  $l=1$  in  $S=2$  (i.e., if  $J^\pi=3^+$ ), or by  $l=2$  in  $S=1$  and/or  $S=2$  (i.e., if  $J^\pi=3^-$ ). One of the purposes of the following analysis (parts B and C) is to determine which of the above assignments to the 7.37-MeV level in  $\text{Be}^{10}$  is the most likely.

The expression for the differential cross section for unpolarized neutrons scattered elastically from nuclei is given by Blatt and Biedenharn<sup>13</sup> [their Eq. (4.6)]. It can be written in the form of Eq. (1) with

$$B_L = \frac{\chi^2}{4(2I+1)(2i+1)} \times \sum (-1)^{s'-s} \bar{Z}(l_1 J_1 l_2 J_2; SL) \bar{Z}(l_1 J_1 l_2 J_2; S'L) \times \text{Re}[(\delta_{S'S} - U_{S'l_1; s l_1}^{J_1})^* (\delta_{S'S} - U_{S'l_2; s l_2}^{J_2})]. \quad (3)$$

Here the  $U$ 's are the elements of the scattering matrix, and it is assumed in the notation of Ref. 13 that (1) the recoil nucleus is not excited in the scattering (i.e.,  $\alpha'=\alpha$ ) and (2) the orbital angular momentum and the spins of the particles do not change between the entrance and exit channels (i.e.,  $l_1'=l_1$ ,  $l_2'=l_2$ ,  $I'=I$ , and  $i'=i$ ).

With the same assumptions, the expression given by Simon and Welton<sup>14</sup> [their Eq. (3.2)] for the differential polarization in the scattering becomes

$$\sigma_p(\theta) \mathbf{n} = \mathbf{n} \sum C_L P_L^1(\cos\theta),$$

where (with  $\hat{i}$ =imaginary unit)

$$C_L = \sum \frac{\sqrt{3}(-1)^{I-i-s+l_1+J_1-s_1'}}{4(2I+1)} (2l_1+1)(2l_2+1)[(2S_1'+1)(2S_2'+1)]^{1/2} \times (2J_1+1)(2J_2+1)(l_1 l_2 00 | L 0)^2 \times W(iS_1' iS_2'; I1)W(l_1 J_1 l_2 J_2; SL) \times X(J_1 l_1 S_1'; J_2 l_2 S_2'; LL1) \chi^2 \times \text{Re}[\hat{i}(\delta_{S_1'S} - U_{S_1'l_1; s l_1}^{J_1})^* (\delta_{S_2'S} - U_{S_2'l_2; s l_2}^{J_2})] \times \left[ \frac{2L+1}{2} \frac{(L-1)!}{(L+1)!} \right]^{1/2} \quad (4)$$

<sup>11</sup> L. Cranberg, Phys. Rev. **114**, 174 (1959).

<sup>12</sup> P. R. Bevington, W. W. Roland, and H. W. Lewis, Phys. Rev. **121**, 871 (1961); A. Smith (private communication).

<sup>13</sup> J. M. Blatt and L. C. Biedenharn, Rev. Mod. Phys. **24**, 258 (1952).

<sup>14</sup> A. Simon and T. A. Welton, Phys. Rev. **90**, 1036 (1953).

and, in accordance with the Basel convention,

$$\mathbf{n} = \frac{\mathbf{k}_i \times \mathbf{k}_f}{|\mathbf{k}_i \times \mathbf{k}_f|},$$

in which  $\mathbf{k}_i$  and  $\mathbf{k}_f$  are the wave vectors of the incident and scattered neutron, respectively. The notation agrees with that of Simon and Welton unless otherwise stated.

Since the levels involved here are very few and well isolated, a single-level expression for the scattering-matrix elements was considered adequate. However, the possibility of channel-spin flip in the exit channel was retained in the problem by using scattering-matrix elements for an arbitrary number of channels. The elements are given by

$$U_{cc'} = \exp[-i(\phi_c + \phi_{c'})] \times \left[ \delta_{cc'} + i \frac{(\Gamma_c \Gamma_{c'})^{1/2}}{(\mathcal{E} + \Delta - E) - \frac{1}{2}i \sum_{c''} \Gamma_{c''}} \right]. \quad (5)$$

In our case the only difference between channels  $c$  and  $c'$  is the channel spin  $S=1$  or  $2$ . The quantities in Eq. (5) are the same as described by Lane and Thomas<sup>15</sup> and also by Vogt,<sup>16</sup> where the  $\phi_c$  and  $\phi_{c'}$  are the magnitudes of the hard-sphere-scattering phase shifts,  $\Gamma_c$  and  $\Gamma_{c'}$  are the natural widths, related through the penetration factor  $\mathcal{P}_l$  to the reduced width  $\gamma_{c'}^2$  by  $\Gamma_{c'} = 2\mathcal{P}_l \gamma_{c'}^2$ ,  $\mathcal{E}$  is the characteristic energy, and  $\Delta$  is the level shift.

### B. The $J^\pi = 3^+$ Assignment for the 7.37-MeV State in Be<sup>10</sup>

As mentioned in Sec. I when only neutron differential scattering data were available, calculations of  $\sigma_u(\theta)$  on the 0.625-MeV resonance assuming  $J^\pi = 3^+$  with  $l=1$  and  $S=2$  (only) were fairly consistent with the data provided that all  $s$ -wave scattering was in  $S=1$ , this latter proviso being somewhat at variance with the scattering data at thermal energies. In the investigation being reported here, more extensive and more exact calculations were made not only for the coefficients in the expansion for  $\sigma_u(\theta)$  but also for those for  $\sigma_p(\theta)$ . From Fig. 4 it is clear that near the 0.625-MeV resonance the dominant resonant behavior in the polarization appears in the term  $C_2$ . If the 7.37-MeV state is formed via  $l=1$  and  $S=2$  only, then from the selection rules on the coupling coefficients the resonant part of the term  $C_2$  can arise only from interference with backgrounds of odd-parity partial waves, the most probable being  $l=1$ . The possible  $J^\pi$  values for the backgrounds are  $0^+$ ,  $1^+$ ,  $2^+$ , and  $3^+$ . Background

<sup>15</sup> A. M. Lane and R. G. Thomas, Rev. Mod. Phys. **30**, 257 (1958).

<sup>16</sup> E. Vogt, in *Nuclear Reactions*, edited by P. M. Endt and M. Demeur (Interscience Publishers, Inc., New York, 1959), Vol. I.

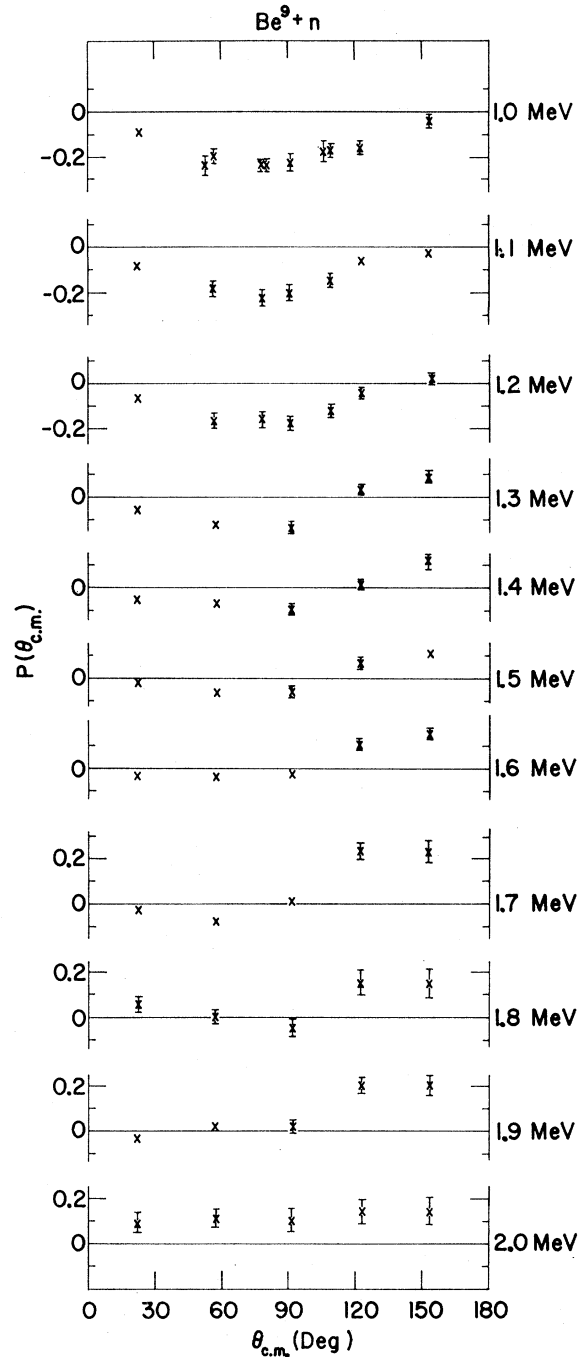


FIG. 3. Angular distribution of the measured polarization of neutrons scattered from Be<sup>9</sup> for neutron energies of 1.0–2.0 MeV.

of  $0^+$  cannot contribute to resonance interference since, for a  $0^+$ -state, the only allowed spin in the entrance and exit channels is  $S=1$ . A  $0^+$ -background would contribute to a nonresonant term in  $C_1$  by interference with the  $s$  waves in  $S=1$ . The  $1^+$ - and  $2^+$ -backgrounds may be formed in  $S=1$  or  $2$  with  $l=1$ , and would contribute to a resonance term in  $C_2$  by interference with the  $3^+$  ( $l=1$ )-resonance. A  $3^+$  ( $l=1$ )-background

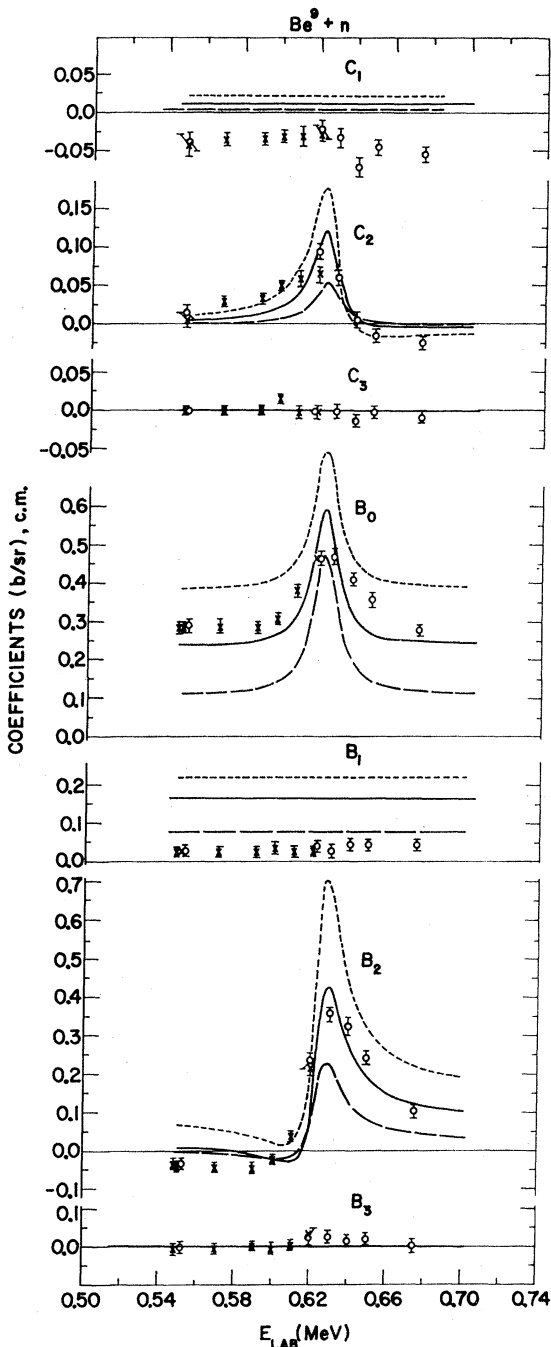


FIG. 4. Variation of the experimental coefficients  $C_L$  and  $B_L$  with neutron energy across the 0.625-MeV resonance as compared with the curves calculated for different values of the nuclear radius  $R$ . Circles are the experimental values for scatterers  $\frac{1}{8}$  in. thick, crosses for a thickness of  $\frac{1}{4}$  in. Curves are calculated for the assignment  $3^+(l=1, S=2)$  only for the state. The long-dash curves are for  $R=5.6$  F, the solid curves for  $R=8$  F, and the short-dash curves for  $R=10$  F.

requires  $S=2$  only, and so does the resonance. No polarization can result from the interference between such a background and the  $3^+(l=1)$ -resonance, since all quantum numbers are the same for both resonance

and background. Therefore, the scattering matrix has only a single element.<sup>10</sup> Thus the resonant behavior of the dominant  $C_2$  term probably comes from the interference of the  $3^+(l=1)$  resonance with both  $1^+(l=1)$ - and  $2^+(l=1)$ -backgrounds.

The coefficients  $B_L$  and  $C_L$  were calculated for this latter case with radii of 5.6, 8.0, and 10.0 F, and with a total natural width for the resonance of approximately 16 keV, a laboratory resonance energy of 625 keV,  $s$ -wave hard-sphere scattering in  $S=1$  only, and the  $1^+$  and  $2^+$ -backgrounds taken as hard-sphere scattering in  $S=1$  and 2. The results were that only for the larger radii of  $R=8$  and 10 F was the calculated  $C_2$  large enough to be comparable in magnitude with that from the data, but the variation of  $C_2$  with energy was opposite to that of the data, i.e., it was a mirror reflection (about the resonant energy) of the variation of the data for  $C_2$ . All of the coefficients  $B_L$  and the coefficient  $C_1$  were also in serious disagreement with the data. Reversing the sign of the background  $1^+$  and  $2^+$  phase shifts reversed the signs of the calculated  $C_2$  terms compared with those from the data. Such reversal of the signs of the phase shifts is equivalent to including broad high-energy states of this character. The agreement with the data was not improved by replacing the  $1^+$  and  $2^+$  potential scattering by broad  $1^+$  and  $2^+$  bound states in which channel-spin flip was included. The spin-flip terms tended to cancel off some of the polarization.

At this point these calculations were repeated with  $\phi_c = \phi_{s1}^J = \phi_{21}^3 = 0$  in Eq. (5) for the channel exciting the resonance, i.e., with  $J^\pi = 3^+, l=1, S=2$ . If the hard-sphere scattering is interpreted as being the net effect of contributions of all the distant levels of this character, then such an effect can be reduced to zero near the 0.625-MeV resonance only if the phase shift includes a strong contribution from a state (other than this one itself) whose phase shift is of the same character but of opposite sign to the hard-sphere phase shift. Such a  $3^+$  state would have to be broad and located at energies above the 7.37-MeV state being considered. Though no such state has yet been reported, such a possibility may be considered in the search for an interpretation of our data.

The results of these calculations with  $\phi_{21}^3 = 0$  are shown in Fig. 4. For  $R=5.6$  F, the resonant terms were again far too small. For  $R=8.0$  F, the terms  $B_0$  and  $B_2$  were in reasonable agreement with the data, but the resonance in the calculated  $C_2$  was not as asymmetric as the one from the data, although the magnitude was more in agreement. Furthermore,  $C_1$  was positive instead of being negative as the data are, and the calculated  $B_1$  was approximately 5-6 times the experimental values.

A number of variations were tried with  $R=8.0$  F. Removing the  $2^+$  background to bring the calculated values of  $C_1$  and  $B_1$  closer to the measured values greatly reduced  $C_2, B_0,$  and  $B_2$  so they disagreed even

worse with the data. However, when it was assumed that the  $1^+$  and  $2^+$   $p$ -wave backgrounds as well as the resonance were in  $S=2$  only and that the  $1^-$   $s$ -wave background was in  $S=1$  only, the terms  $B_1$  and  $C_1$  went to zero while  $C_2$  remained unchanged. The nonresonant part of  $B_0$  became smaller so that it was in greater disagreement with the data while the fit for  $B_2$  was improved. At this point the  $s$ -wave phase shift might be increased in magnitude (e.g., because of the bound  $1^-$  state at  $E_{\text{ex}}=5.96$  MeV) in order to raise the nonresonant part of  $B_0$ . But even if this phase shift were increased to its maximum of  $90^\circ$ ,  $B_0$  would only be increased by 0.02 and the calculated  $B_0$  would still remain much smaller than the data. None of these variations seemed to improve the fit.

Possible effects near 625 keV of the resonance at 815 keV were included in these calculations for  $R=8.0$  F by assuming  $J^\pi=2^+(l=1)$  for the latter resonance. These effects on the coefficients  $C_L$  and  $B_L$  at energies near the 625-keV resonance were found to be too small to plot on Fig. 4, so that the 815-keV resonance can be neglected in these calculations. Possible contributions from the broad  $2^+$  state in  $\text{Be}^{10}$  at  $E_{\text{ex}}=9.4$  MeV were also considered, but these reduce  $C_2$ ,  $B_0$ , and  $B_2$  to values below the experimental values.

For a very large radius of 10 F, with  $s$  waves in  $S=1$  only and  $1^+$  and  $2^+$   $p$  waves in  $S=1$  and 2 (as in the first case for  $R=8$  F),  $C_2$  appeared to agree quite well with the data as seen in Fig. 4 when one considers the energy spread of the beam. However,  $C_1$  and all the  $B_L$  were in complete disagreement with the data, in some cases by orders of magnitude. The same variations of parameters and assumptions were made for this radius as for  $R=8$  F, the results were similar but more exaggerated.

Finally, the inclusion of  $s$ -waves in channel spin 2 so that a more reasonable radius of 5.6 F could be used to fit the nonresonant  $B_0$  gives very large resonant and nonresonant terms in both  $C_1$  and  $B_1$ , in sharp disagreement with the data. The measured  $B_1$  shows no such resonance term and what little variation there is in  $C_1$  across the resonance amounts to only 10% or so of that calculated. Also the nonresonant terms in  $B_1$  and  $C_1$  (arising because the  $p$  waves of the  $1^+$  and  $2^+$  states interfere with the  $s$  waves in  $S=2$ ) have large positive values and disagree with the data.

In summary then, we were not able to fit all of the  $B_L$  and  $C_L$  simultaneously for the  $3^+$  ( $l=1$ ) assignment to the 7.37-MeV state in  $\text{Be}^{10}$ . Furthermore, even the best fits possible required some rather unusual and to some extent unjustified assumptions: (1) all  $s$ -wave scattering is in channel spin  $S=1$  only, an assumption that does not agree with scattering data at thermal energies; (2) the radius has the very large value 8.0 or 10.0 F, neither value being at all realistic; and (3)  $\phi_{21}^3=0$  for the assumed resonant  $p$ -wave channel, an improbable value for these large radii. It should be understood that these attempts to fit the data with a

theoretical expression do not exhaust all the combinations of states and parameters possible in such a complex problem. There may indeed be other possibilities and variations that might possibly fit the data for a  $3^+$  ( $l=1$ ) assignment. However, these calculations based on the simpler and more probable situations did not represent the data on  $\sigma_T$ ,  $\sigma_u(\theta)$ , and  $\sigma_p(\theta)$  for this assignment.

### C. The $3^-$ ( $l=2$ ) Possibility for the 7.37-MeV State

If this state has negative parity, then it can be formed with even  $l$ , the lowest of which is  $l=2$  for this case. Values  $l \geq 3$  were neglected. The assumption of  $d$ -wave formation (and decay) allows both channel spins  $S=1$  and 2 to enter. From the selection rules for the coupling coefficients, terms as high as  $B_4$  and  $C_4$  are possible in Eqs. (1) and (2), respectively. The data, however, show that the coefficients  $B_L$  and  $C_L$  for  $L \geq 4$  are zero within the experimental error for all energies involved in this measurement. The experimental fact that  $B_4=0$  requires that  $\Gamma_{12}^3$  and  $\Gamma_{22}^3$  ( $\Gamma_c = \Gamma_{Sl}^J$ ) in Eq. (5) are *very* nearly equal; otherwise the  $B_4$  calculated from Eq. (3) would be resonant and large enough to be observed experimentally. From angular momentum considerations the coefficient  $C_4$  could only arise from interference between those terms representing channel-spin flip and those for no-flip in the decay of the state by  $d$  waves. If  $\phi_{12}^3 = \phi_{22}^3 = 0$  ( $\phi_c = \phi_{Sl}^J$ ) in Eq. (5) for this state, then the channel-spin-flip term in  $C_4$  (and hence  $C_4$  itself) becomes zero in agreement with the data. At these energies the  $d$ -wave hard-sphere phase shifts  $\phi_{12}^3$  and  $\phi_{22}^3$  are indeed very small compared with those for  $s$  and  $p$  waves, so this assumption was made in all calculations for this case.

As mentioned above, the dominant coefficients near the 0.625-MeV resonance are  $B_0$ ,  $B_2$ , and  $C_2$ . With  $d$ -wave formation,  $C_2$ , and the resonant part of  $B_2$  arise from interference with the  $s$ -wave background. Since thermal scattering data show no channel-spin dependence, the hard sphere potential phase shifts for  $s$  waves [ $\phi_{10}^1$  and  $\phi_{20}^2$  in Eq. (5)] were taken to be equal to each other. The magnitude of this phase shift was obtained for a radius of 5.6 F, and the results calculated from it fit the  $s$ -wave background well at 0.625 MeV. The pronounced rise in  $B_0$ , shown in Fig. 5 at energies below about 0.5 MeV, strongly suggests an added contribution to  $\sigma_T$  from bound states of the character  $1^-$  and/or  $2^-$  which are formed by  $s$ -waves in  $S=1$  and/or 2, respectively. Two such states have in fact been reported<sup>17</sup> in  $\text{Be}^{10}$  just below the neutron binding energy. Because information on the widths of such levels is vague, values of level positions and widths were chosen such that the combined effect of  $s$ -wave hard-sphere

<sup>17</sup> F. Ajzenberg-Selove and T. Lauritsen, Nucl. Phys. 11, 1 (1959).

and *s*-wave bound-state scattering reproduced most of the energy dependence of  $B_0$  below 0.5 MeV. A characteristic energy  $\mathcal{E} = -0.2$  MeV and a reduced width  $\gamma^2 = 0.05$  MeV for the  $1^-$  and the  $2^-$  states were found to fit the data fairly well and were used in the final calculations. Since this experiment senses only the distant effects of such bound levels, the positions and widths employed in this analysis are intended only to give the approximate equivalent effect of the levels

at a distance and are not necessarily the exact values.

If the 0.625-MeV resonance is assumed to be  $3^-(l=2)$ , formed equally in  $S=1$  and  $2$ , the calculated coefficients  $C_L$  and  $B_L$  near the resonance are as shown by the solid curves in Fig. 6. The inset in Fig. 6 shows an estimate of the energy distribution in the neutron beam. The dashed curves are the mean values of the calculated  $C_L$  and  $B_L$  with respect to this energy distribution function. The calculated  $C_2$ ,  $B_0$ , and  $B_2$  are

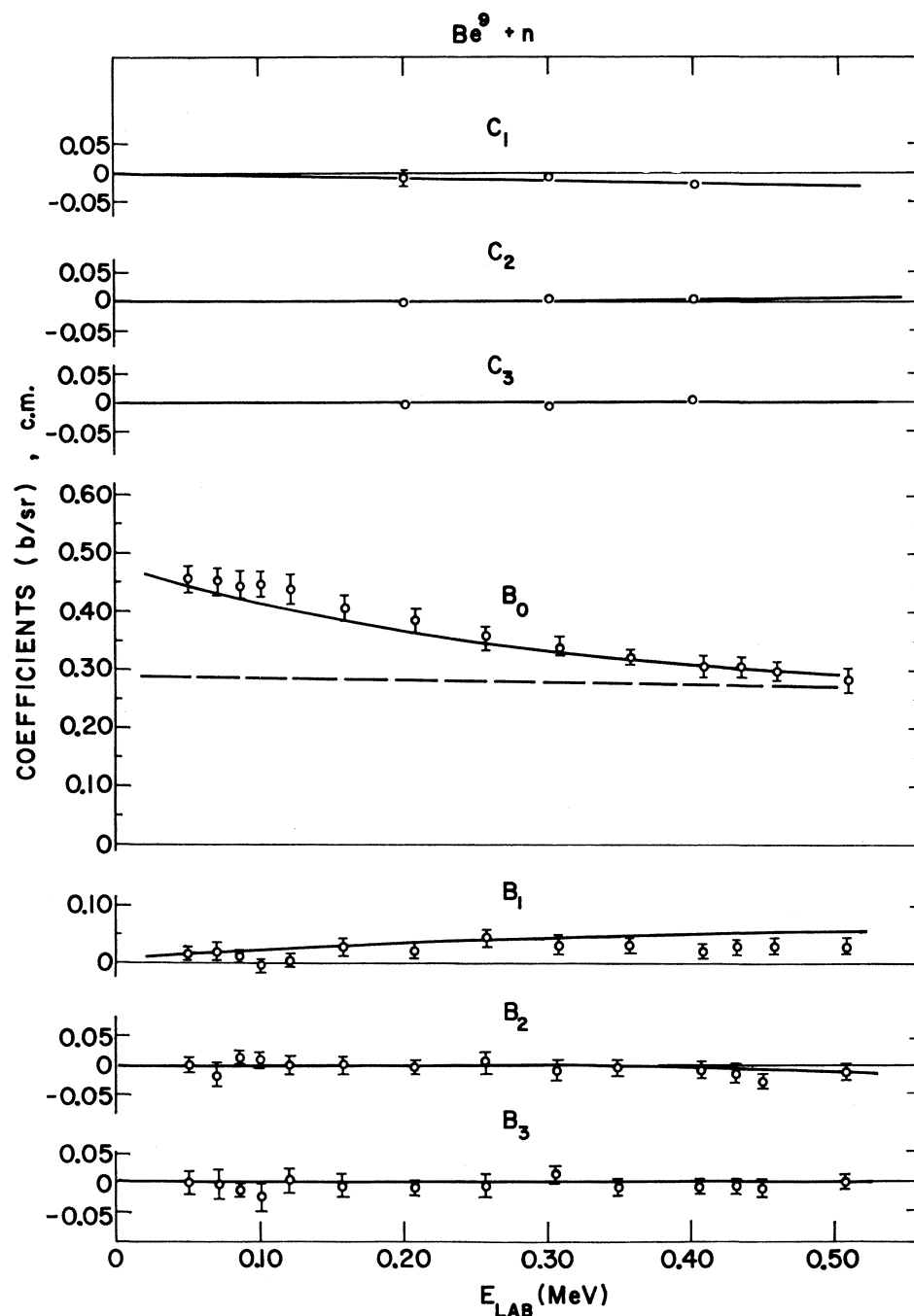


FIG. 5. Variation of the coefficients  $C_L$  and  $B_L$  with neutron energy below 0.5 MeV. The scatterer was  $\frac{1}{8}$  in. thick. All experimental points at 0.20, 0.30, and 0.40 MeV are from the present experiment. The additional points for the  $B_L$  are taken from Ref. 8. The solid curves were calculated from the final set of parameters shown in Table I. No averaging over energy spread was necessary since all coefficients are slowly varying here. The dashed curve in  $B_0$  is calculated without considering any effects of bound states.



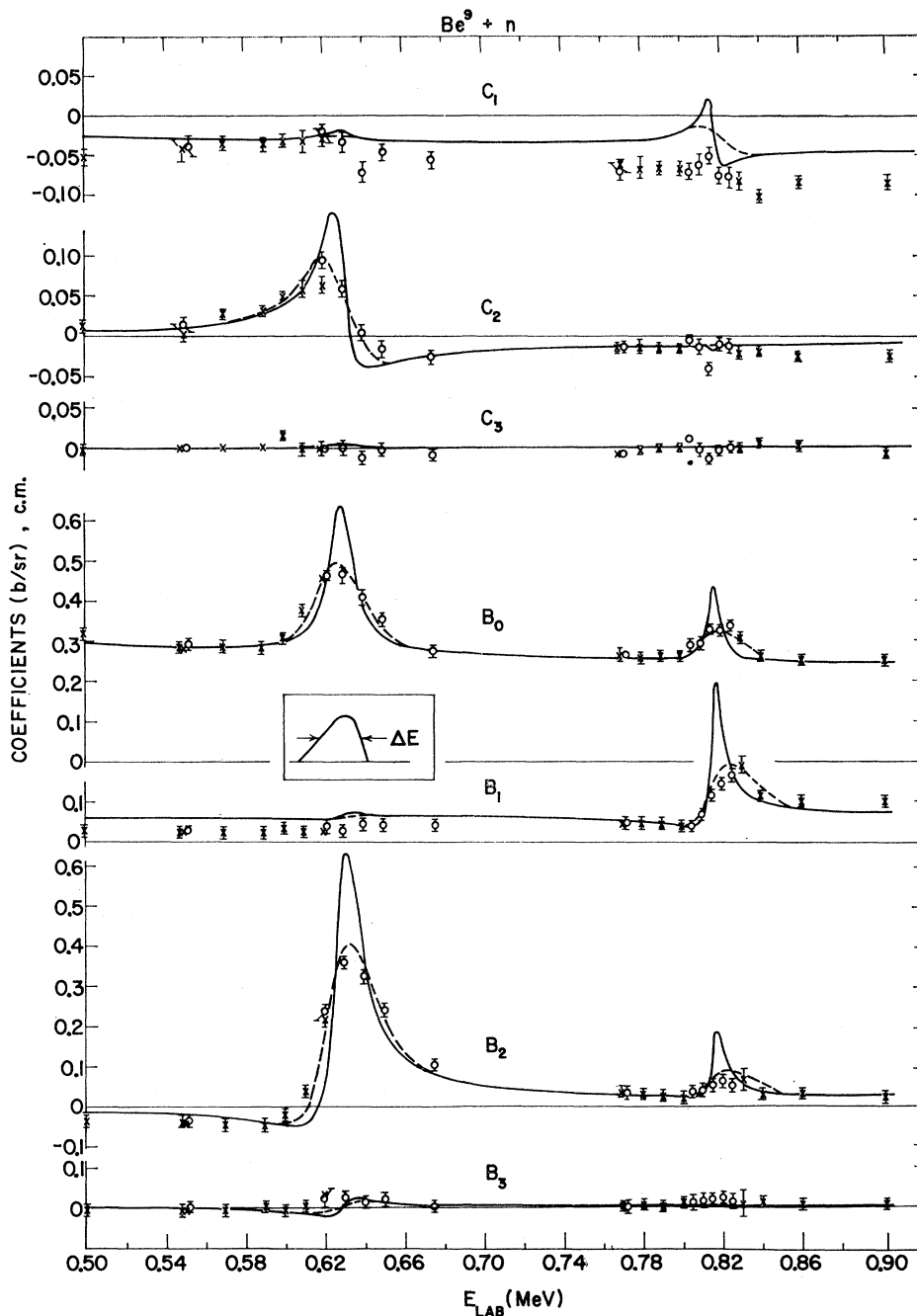


FIG. 6. Variation of the experimental coefficients  $C_L$  and  $B_L$  with neutron energy over the region of the two resonances. Circles and crosses are experimental values for scatterers  $\frac{1}{16}$  in. and  $\frac{1}{8}$  in. thick, respectively. The solid curves were calculated from the final set of parameters shown in Table I, the assignment for the 0.625-MeV resonance being  $3^-$  ( $l=2$ ) and that for the 0.815-MeV resonance being  $2^+$  ( $l=1$ ). The estimated distribution of energies in the beam is shown in the inset. Dashed curves were obtained by averaging the calculated curves over the energy distribution of the beam.

seen to agree well with the data. The width  $\Gamma=16$  keV chosen for these calculations is somewhat narrower than the value  $\Gamma=25$  keV found by Willard *et al.* but was more consistent with our data for the  $J=3$  assignment. In addition, Hibdon,<sup>18</sup> who used a very narrow energy spread in a preliminary measurement of the transmission cross section  $\sigma_T$ , found  $\Gamma \approx 16$  keV. The broad energy spread in our work introduces some

<sup>18</sup> C. T. Hibdon (private communication).

error into the determination of the width, but it appears to be smaller than 25 keV. For a radius of 5.6 F, the quantity  $\theta^2 = 2\mu R^2 \gamma^2 / 3\hbar^2$  is 0.075 for the parameters used in the calculations with the  $3^-$  ( $l=2$ ) assignment.

Up to this point the even-parity partial waves have been taken into account rather well. The effects of odd-parity partial waves will now be included. The terms  $B_1$  and  $C_1$  result from the interference between partial waves of opposite parity. With the  $s$ - and  $d$ -wave contributions remaining the same as already

described, various assumptions were made for the possible  $p$ -wave contributions. Underlying the resonance effects there is a background of  $C_1$  and  $B_1$  which varies slowly with energy. Attempts were made to fit simultaneously the  $B_1$  and  $C_1$  backgrounds by including  $p$ -wave potential scattering and  $p$ -wave resonance scattering from states with  $J^\pi=0^+, 1^+, 2^+$ , and  $3^+$ . Broad bound states and broad states at high energies were assumed. For the  $0^+$  assumption, reasonable agreement with  $B_1$  could be obtained; but the values calculated for  $C_1$  were too small by an order of magnitude or their signs were opposite those of the data. While some  $0^+$  effect might well be present, it is not the dominant one in the  $C_1$  background. For backgrounds of the characters  $1^+$  and  $2^+$  ( $S=1$  and  $2$  for each), the calculated values of  $C_1$  have roughly the magnitudes of the measured values but the opposite sign; and the values of  $B_1$  are again in reasonable agreement with the data. Reasonable agreement with the experimental  $C_1$  could be obtained only for the case of an angular momentum and parity assignment of  $3^+$  for the background scattering. When only potential scattering ( $U_{cc}=U_{sl}J = \exp[-\phi_{21}^3]$ ) was used for this background, the calculated values were in closer agreement with the data.  $B_1$  was slightly larger and  $C_1$  slightly smaller than the experimental values. These results for  $B_L$  and  $C_L$  are shown in Fig. 6. Adding a broad bound  $3^+$  state to this background gave better agreement with  $C_1$  but serious disagreement with  $B_1$ . When the bound  $3^+$  state was replaced by a broad state at high energy, the result was the converse, i.e., better agreement with  $B_1$  but serious disagreement with  $C_1$ . The reason for this inability to fit the slowly varying backgrounds of both  $B_1$  and  $C_1$  simultaneously is not clear. The present discrepancies may be due to the combined effects of several broad or distant levels and/or some other type of interaction.

In summary, the calculated curves in Figs. 4 and 6 strongly favor the assignment  $J^\pi=3^-$  over  $J^\pi=3^+$  for this resonance.

#### D. The 7.54-MeV State in $\text{Be}^{10}$ and Other Considerations

The parity of the resonance at a neutron energy of 0.815 MeV, which corresponds to the 7.54-MeV state in  $\text{Be}^{10}$ , has not been established previously. If the experimental behavior of  $B_1$  in the vicinity of this resonance is compared with the behavior near the 0.625-MeV resonance, it can be concluded that the parity of the 0.815-MeV resonance is positive and that the state is most probably formed via  $l=1$ . The background phase shifts are not much different at the two resonances, and the values of  $B_1$  result from the interference between phase shifts of opposite parity. Therefore the fact that  $B_1$  is resonant at 0.815 MeV and not at 0.625 MeV strongly implies that the parity of the former is positive since we concluded in Sec. C that the resonance at 0.625 MeV and the dominant backgrounds have negative parities.

TABLE I. Level parameters for the calculated curves shown in Figs. 1, 2, 5, and 6 with  $R=5.6$  F.

$E_r$ MeV, (lab)	$J^\pi$	$l$	$\xi$ MeV, (c. m.)	$\gamma_{n^2}$ (MeV, c. m.)		$\Gamma_n(E_r)$ (MeV, lab)		$\theta^2$
				$S=1$	$S=2$	$S=1$	$S=2$	
0.625	$3^-$	2	0.287	0.082	0.082	0.008	0.008	0.075
0.815	$2^+$	1	0.732	0.0008	0.0053	0.0008	0.0053	0.0028

A strong argument, however, can be made in favor of positive parity for the 0.815-MeV resonance quite independently of the 0.625-MeV one. Since the off-resonance angular distribution in this general area is isotropic (i.e.,  $B_0 \gg B_1, B_2,$  or  $B_3$ ) the background must contain  $s$ -wave phase shifts large compared with those of higher  $l$  values. The dominant resonant term in the data at 0.815 MeV is  $B_1$ . Such a pronounced variation in  $B_1$  would indeed result from the interference between a resonance with  $l=1$  and a dominant background with  $l=0$ . This again strongly indicates that the state is formed by  $l=1$  interaction and therefore has positive parity. It might be argued that this is a  $d$ -wave resonance, but it is much less likely that such large  $B_1$  values are produced by interference between  $d$  waves and the smaller background  $p$  waves.

This resonance was included in the calculations shown in Fig. 6 on the assumption that the character of the state was  $J^\pi=2^+$ . The peak in the total cross sections of Willard *et al.* was too high for  $J=0$  or  $1$ . They concluded, therefore, that  $J=2$  and  $\Gamma=8$  keV for this resonance. We calculated the coefficients  $B_L$  and  $C_L$  for both possibilities,  $J^\pi=2^+$  and  $J^\pi=3^+$ . There is little qualitative difference between the two results, but most terms are larger for  $3^+$ . Since the energy spread of our neutron beam had a half-width of about 20 keV, we were unable to distinguish clearly between these two possibilities. Assuming  $J=2$ , we find that a slightly smaller width  $\Gamma \approx 6$  keV ( $\theta^2=0.0028$ ) is more consistent with our data. A considerable error in the determination of the ratio of partial widths for this state in channel spins 1 and 2 is introduced because of the large energy spread in the beam. To illustrate this, initial calculations employed a ratio of unity. Final calculations with a ratio  $\Gamma_{21}^2/\Gamma_{11}^2=6.6$  gave only slightly better agreement with the data. However, such an uncertainty does not play an important role in the parity assignment of this state. The broad  $2^+$  state in  $\text{Be}^{10}$  at  $E_{\text{ex}}=9.4$  MeV might affect neutron scattering at energies below 1 MeV, but calculations showed that any such contribution would be small.

The final parameters for the scattering resonances, as used to obtain the curves in the figures, appear in Table I. At energies from 0.02 to 0.50 MeV the coefficients  $B_L$  and  $C_L$  were also calculated with these final parameters. Comparison with the data displayed in Fig. 5 shows that the results of the calculations are in agreement with the data at low energies also. For

comparison with the experimental data in the form of angular distributions, the values of  $\sigma_u(\theta)$  and  $P(\theta)$  calculated with the final parameters are included in Figs. 1 and 2.

No attempt has been made here to fit the experimental data for  $P(\theta)$  and  $\sigma_u(\theta)$  for energies from 1 to 2 MeV. Fitting the data in this region may well lead to a better explanation of the background effects below 1 MeV. In the region from 1 to 2 MeV, the  $B_L$  and  $C_L$  are slowly varying functions of energy so that it is very difficult to obtain a unique solution with the many free parameters available here. When measurements similar to these are extended to neutron energies well above the resonances near 2.9 MeV, it may be more attractive to extend the analysis to energies above 1 MeV.

### CONCLUSIONS

From the measurements and interpretations discussed above, the following conclusions can be drawn:

(a) The resonance behaviors of the  $B_L$  and  $C_L$  near the 0.625-MeV resonance favor the assignment  $3^-$  ( $l=2$ ) rather than  $3^+$  ( $l=1$ ).

(b) The partial widths in  $S=1$  and 2 for this state must then be nearly equal.

(c) The resonant behavior near the 0.815-MeV resonance is (except for one point for  $C_2$ ) consistent with an assignment of  $J=2$  and implies positive parity with  $l=1$ .

(d) The nonresonant background contributing to  $B_1$  and  $C_1$  are best fitted by the assumption that the  $p$ -wave background is dominated by  $J^\pi=3^+$ , though none of the possibilities considered here could simultaneously fit both  $B_1$  and  $C_1$  very well.

(e) At energies below 500 keV, the variations of  $B_L$  and  $C_L$  with energy are reasonably well reproduced by the inclusion of the known  $1^-$  and  $2^-$  bound states.

(f) A radius of 5.6 F for this interaction gives reasonable agreement with the data.

### ACKNOWLEDGMENTS

The authors wish to thank Dr. J. E. Monahan for useful discussions, and to express their appreciation to W. Ray, R. Amrein, and the crew of the Argonne 4.5-MeV Van de Graaff for their assistance in the experiment and to D. Mueller and R. Obenchain for aid in data reduction.